



# HHS Public Access

Author manuscript

*Environ Sci Technol Lett.* Author manuscript; available in PMC 2020 December 03.

Published in final edited form as:

*Environ Sci Technol Lett.* 2019 March 12; 6(3): 119–125. doi:10.1021/acs.estlett.9b00031.

## Phospholipid Levels Predict the Tissue Distribution of Poly- and Perfluoroalkyl Substances in a Marine Mammal

Clifton Dassuncao<sup>†,‡,\*</sup>, Heidi Pickard<sup>†</sup>, Marisa Pfohl<sup>§</sup>, Andrea K. Tokranov<sup>†</sup>, Miling Li<sup>†</sup>, Bjarni Mikkelsen<sup>||</sup>, Angela Slitt<sup>§</sup>, Elsie M. Sunderland<sup>†,‡</sup>

<sup>†</sup>Harvard John A. Paulson School of Engineering and Applied Sciences, Harvard University, Cambridge, MA, USA 02138

<sup>‡</sup>Department of Environmental Health, Harvard T.H. Chan School of Public Health, Harvard University, Boston, MA, USA 02115

<sup>§</sup>Biomedical and Pharmaceutical Sciences, University of Rhode Island, Kingston, RI, USA 02881

<sup>||</sup>Museum of Natural History, To shavn, Faroe Islands 188

### Abstract

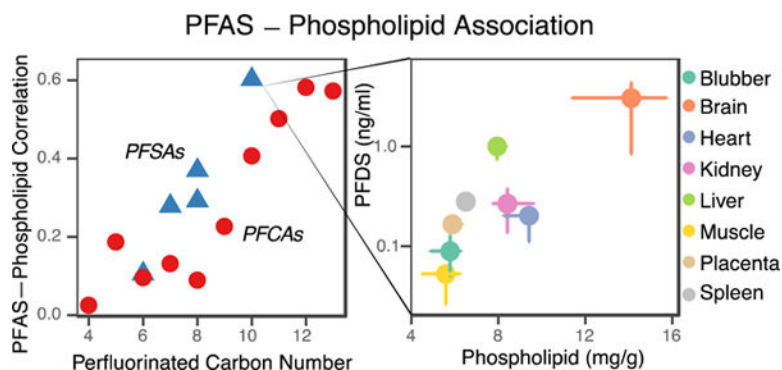
Exposure to poly- and perfluoroalkyl substances (PFASs) has been linked to many negative health impacts in humans and wildlife. Unlike neutral hydrophobic organic pollutants, many PFASs are ionic and have been hypothesized to accumulate in both phospholipids and protein-rich tissues. Here we investigate the role of phospholipids for PFAS accumulation by analyzing associations among concurrent measurements of phospholipid, total protein, total lipid and 24 PFASs in the heart, muscle, brain, kidney, liver, blubber, placenta and spleen of North Atlantic pilot whales (*Globicephala melas*). The sum of 24 PFASs ( $\sum_{24}\text{PFAS}$ ) was highest in the liver (median 260 ng g<sup>-1</sup>; interquartile range (IQR) 216–295 ng g<sup>-1</sup>) and brain (86.0; IQR 54.5–91.3 ng g<sup>-1</sup>), while phospholipid levels were highest in brain. The relative abundance of PFASs in the brain greatly increases with carbon chain lengths of 10 or greater, suggesting shorter-chained compounds may cross the blood-brain barrier less efficiently. Phospholipids were significant predictors of the tissue distribution of the longest-chained PFASs: perfluorodecanesulfonate (PFDS), perfluorododecanoate (PFDoA), perfluorotridecanoate (PFTrA), and perfluorotetradecanoic acid (PFTA) ( $r_s = 0.5\text{--}0.6$ ). In all tissues except the brain, each 1 mg g<sup>-1</sup> increase in phospholipids led to a 12%–25% increase in the concentration of each PFAS. We conclude that partitioning to phospholipids is an important mechanism of bioaccumulation for long-chained PFASs in marine mammals.

### Graphical Abstract

\*Corresponding Author cld292@mail.harvard.edu.

#### Supporting Information

This information is available free of charge on the ACS Publications website: Details on PFAS analysis, protein analysis, lipid analysis, statistical analysis and relation to bioaccumulation, list of PFASs monitored, method detection limits, summary statistics of measurements.



## 1 Introduction

Human exposure to poly- and perfluoroalkyl substances (PFASs) has been associated with metabolic disruption, immunotoxicity, and cancer.<sup>1, 2</sup> Many PFASs have long environmental lifetimes and bioaccumulate in aquatic food webs.<sup>3, 4</sup> As a result, seafood consumption is an important human exposure pathway.<sup>5</sup> Hydrophobic persistent organic pollutants are known to accumulate in neutral storage lipids.<sup>6</sup> However, factors controlling the bioaccumulation and tissue distribution of different PFASs are not fully understood.<sup>7–9</sup>

Perfluoroalkyl acids (PFAAs), an important subclass of PFASs, are anionic under environmentally relevant conditions and accumulate in certain protein-rich tissues such as blood and liver.<sup>10–12</sup> Two mechanisms for PFAA accumulation have been proposed in prior work: (1) partitioning to phospholipids<sup>8, 13</sup> and (2) binding to specific proteins.<sup>9</sup> Both phospholipids and PFAAs contain a hydrophilic head and a hydrophobic tail. The phospholipid model proposes that cell membranes, which are composed of phospholipids, act as a significant sink for PFAAs.<sup>13</sup> Phospholipid-water partition coefficients and related proxies thus provide a potential screening metric for bioaccumulation of organic ions.<sup>14–16</sup>

Here we investigate whether the phospholipid content of marine mammal tissues can be used to predict PFAS accumulation. We hypothesize that correlations between phospholipid content and PFAS concentrations will vary based on their functional group and carbon chain-length.<sup>17, 18</sup> We further hypothesize that structural proteins and storage lipids act as significant sorption compartments for neutral or semi-neutral PFASs. We test these hypotheses using concurrent measurements of 24 PFASs, total phospholipids, total lipids, and total protein concentrations across multiple organ tissues in seven North Atlantic pilot whales (*Globicephala melas*). We use these data to better understand factors affecting PFAS accumulation and partitioning among mammalian tissues.

## 2 Materials and Methods

Long-finned pilot whale samples were collected by the Faroese Natural History Museum in the summer of 2016. Samples were stored frozen at  $-20^{\circ}\text{C}$  at the Faroese Museum of Natural History. We subsampled available tissues, including muscle, heart, kidney, liver, brain, and blubber from each whale. For a subset of whales, placenta ( $n=4$ ) and spleen ( $n=2$ )

were also collected. Blood samples were not available for analysis, and tissue samples were not exsanguinated prior to being frozen and analyzed.

Tissue samples were analyzed for 24 PFASs at Harvard University following established methods for extraction and quantification of PFASs as previously described in Weber et al.<sup>19</sup> and Zhang et al.<sup>20</sup> Total protein was quantified with a Bio-Rad DC Protein Assay kit.<sup>21</sup> Total protein in these tissues reflects the most prevalent type of protein (structural proteins). Lipid extraction was based on the Folch method.<sup>22</sup> Phospholipid levels were quantified with an EnzyChrom™ Phospholipid Assay Kit (EPLP-100) from BioAssay Systems. Additional details on PFAS, protein, and phospholipid analyses are available in the Supporting Information (SI).

Repeated tissue measurements within a whale violate assumptions of independence in a traditional regression. Therefore, we developed a mixed-effects regression model (Equation S1) to quantify the importance of phospholipids, total protein, and total lipid partitioning for PFAS accumulation. We conducted sensitivity analyses to consider individual tissue level effects related to specific protein binding and membrane permeability. For these analyses, we compared model results using measurements from all tissues to models that removed observations from selected tissue types. This avoids confounding from processes related to specific protein binding in the liver and effects of the blood-brain barrier on accumulation in the brain. Further details of statistical analyses can be found in the SI.

### 3 Results and Discussion

#### 3.1 Tissue specific concentrations

Figure 1 shows measured tissue specific concentrations of phospholipids, total protein, total lipids, and the sum of 24 PFASs ( $\sum_{24}\text{PFAS}$ ). Concentrations of the  $\sum_{24}\text{PFAS}$  s do not vary with the same pattern as total protein, total lipid, or phospholipids across tissues (Figure 1, Table S3). Significantly higher concentrations of  $\sum_{24}\text{PFAS}$  s were found in the liver (median 260 ng g<sup>-1</sup>, interquartile range (IQR) 216–295 ng g<sup>-1</sup>) compared to all other tissues, and lowest concentrations were present in muscle (20.5 ng g<sup>-1</sup>, IQR 12.9–23.9 ng g<sup>-1</sup>) and blubber (13.9 ng g<sup>-1</sup>, IQR 13.3–14.5 ng g<sup>-1</sup>) (Figure 1A). Phospholipids were significantly higher in the brain compared to all other tissues (Figure 1B). Total protein was not statistically different across the liver, kidney, muscle, spleen and placenta (Figure 1C). Total lipids were significantly higher in blubber compared to all other tissues (Figure 1D).

#### 3.2 Variability across PFASs and tissues

PFOS, FOSA, and PFCAs with 9 to 14 carbons (C9-C14) were consistently the most abundant PFASs across tissues (Figure 2A). PFOS accounted for 9% of  $\sum_{24}\text{PFAS}$  in the brain and 18–26% in all other tissues. C9-C14 PFCAs accounted for between 39% of  $\sum_{24}\text{PFAS}$  in blubber to 72% in the brain. PFTrA alone represented 43% in the brain and between 10% and 28% in the remaining tissues. The sulfonate with the longest carbon chain, PFDS, made up 4% of  $\sum_{24}\text{PFAS}$  in the brain and <1% in other tissues. The contribution of the semi-neutral precursor FOSA to  $\sum_{24}\text{PFAS}$  ranged from 7% in liver to 25% in muscle. A

higher proportion of C9-C14 PFCAs observed in the brain may reflect differential transport of specific PFASs across the blood-brain barrier and/or differences in the amount and types of binding proteins in cerebral spinal fluid (CSF) compared to whole blood. These findings are consistent with results from Wang et al.<sup>23</sup> that showed varying efficiencies for PFASs crossing the blood-brain barrier in humans, although this study did not reliably detect long-chained compounds.

Figure 2B shows differences in the distribution of individual PFASs based on their carbon chain length and functional group. Phospholipid levels are greatest in the brain. There, the longest chained compounds (PFDS, PFTTrA, PFTA) are proportionally more abundant compared to other tissues (Figure 1). The highest concentrations of C9-C12 PFCAs, PFOS, and FOSA are in the liver. Concentrations in the liver are highest for PFUnDA (C11) and decrease for compounds with shorter and longer carbon chains. An exception to this pattern is for PFHxA, which is almost exclusively present in the liver (Figure 2, Table S3).

The liver contains high concentrations of specific proteins, such as liver fatty acid binding protein (L-FABP). Prior work shows L-FABP efficiently binds PFASs.<sup>24-26</sup> Liver is also the site of albumin production in mammals, another specific protein that has been associated with PFASs.<sup>27-29</sup> The accumulation of PFHxA in the liver may thus reflect a specific affinity for these proteins. Alternatively, since the liver is the primary site of metabolism, elevated levels of PFHxA in this tissue may represent high exposure to precursor compounds. Urban runoff, wastewater, and aqueous film-forming foams (AFFF) have all been shown to contain a large fraction of precursor compounds that oxidize to PFHxA.<sup>30-33</sup> Quantifying total precursors in ocean water or in tissues may clarify the source of the observed liver levels in marine biota.

### 3.3 Association among PFASs, phospholipids, total lipid, and total protein

Figure 3A shows strong correlations among PFASs with similar chain-length (i.e., spearman correlation  $r_s = 0.98$  for PFTA and PFTTrA). PFASs are more correlated with PFCAs of greater chain length. For example, the distribution of PFOS was most similar to PFDA ( $r_s = 0.97$ ), a PFCA with two more carbons, and PFDS exhibited the highest correlation with PFTA, which has four more carbons. This is consistent with current understanding of the varying affinities of PFASs for partitioning to phospholipid bilayers compared to PFCAs.<sup>18, 33</sup>

The longest-chained perfluoroalkyl acids (PFDS, PFDoA, PTrDA, PFTA) are significantly correlated with phospholipid content ( $r_s = 0.50$  to  $0.60$ ) (Figure 3A). The most highly correlated compound is PFDS and this relationship is driven by the high phospholipid levels measured in the brain (Figure 3B). A pattern of decreasing correlation with phospholipid levels with shorter chain-length PFASs is also observed (Figure 3A). By contrast, most other compounds were significantly correlated with total protein levels. The strongest positive association with protein content was observed for PFNA ( $r_s = 0.58$ ). The negative correlation between PFASs and lipid content is driven by low PFAS concentrations but high lipid levels in blubber. Different patterns of correlation across compounds points towards multiple mechanisms of accumulation.

Results from mixed regression models (Table 1) show a pattern consistent with the univariate correlations (Figure 3A). The best model with all tissues shows significant associations with phospholipids for C11-C14 PFCAs, PFDS and FOSA. The strongest association is with PFDS. For each 1 mg g<sup>-1</sup> increase in phospholipids there is a 26% increase in PFDS. Comparatively weaker but significant protein associations are apparent across all compounds except PFHxS (1–2% change in PFAS per mg/g increase in protein). No model retained a lipid association as significant.

PFASs with greater numbers of carbons are more strongly associated with tissue phospholipid content (Figure 3A and Table 1 model with all tissues). PFDS and PFOS are more strongly associated with phospholipids than their corresponding PFCAs. These patterns are consistent with accumulation that is driven by both the hydrophobic forces from the fluorinated tail and ionic forces from the polar headgroup. These patterns are also similar to the relative bioaccumulation potential reported for different PFASs,<sup>3</sup> suggesting that phospholipid partitioning may be a primary mechanism of bioaccumulation in marine mammals.

### 3.4 Longest chained compounds pass blood-brain barrier

Because PFAS measurements in the brain appear to be driving the correlation with phospholipids (Figure 3B), we removed these observations as a sensitivity analysis for the mixed-effects regression model (Table 1). The resulting association with phospholipids is significant for all compounds except PFHpA (Table 1, model without brain). This model indicates, each 1 mg g<sup>-1</sup> increase in phospholipids leads to a 12%–25% increase in PFAS concentration (Table 1). These results demonstrate the robustness of the phospholipid association for the longest-chained PFASs and suggest that differing patterns of accumulation in brain tissue are confounding the association for the shorter-chained PFASs.

The effect of the blood-brain barrier on PFAS accumulation is captured by differences between the two mixed-effect regression models (with and without brain measurements, Table 1). Compounds with less than 10 perfluorinated carbons are not associated with phospholipids in the model that includes brain measurements. This suggests that the shorter-chained compounds may not efficiently cross the blood-brain barrier and/or there are significant differences in the types and levels of proteins in the brain that bind PFASs compared to other tissues. These results are consistent with elevated levels of long-chained PFASs that have been observed in the brain of other mammals.<sup>11, 12</sup> Our modeling approach suggests C12-C14 PFCAs and PFDS may cross the blood-brain barrier through a process mediated by an association with phospholipids.

These results have important implications for the mechanisms of accumulation and toxicity of long-chained PFASs. For example, in vitro studies have shown that PFOS can increase the permeability of the blood-brain barrier.<sup>34</sup> A study of paired cerebral spinal fluid and serum samples in humans found that penetration of PFCAs across the blood-brain barrier increased with chain-length.<sup>23</sup> An increase in carbon chain-length has also been associated with a decrease in neuron viability in rats<sup>35</sup> and altered brain activity in polar bears.<sup>36</sup>

### 3.5 Implications for bioaccumulation

In the simplest case, ignoring metabolism and kinetics, the ability of tissue to accumulate a compound can be described by its sorption capacity,  $K_{BW}$  (Equation 1).<sup>37–39</sup> The total sorption capacity will be dependent on: (1) the relative volume fractions of each sorption compartment: storage lipids ( $f_{SL}$ ), phospholipids ( $f_{PL}$ ), structural proteins ( $f_{SP}$ ), and binding proteins ( $f_{BP}$ ); and (2) the affinity of each compound for each sorption compartment described by their respective partition coefficients ( $K_{SL,W}$ ,  $K_{PL,W}$ ,  $K_{SP,W}$ ,  $K_{BP,W}$ ). For hydrophobic POPs, the octanol-water partition coefficient  $K_{OW}$  is used as a surrogate for  $K_{SL,W}$  and dominates Equation (1).

$$K_{BW} = \frac{C_{PFAS}}{C_{Water}} = K_{SL,W}f_{SL} + K_{PL,W}f_{PL} + K_{SP,W}f_{SP} + K_{BP,W}f_{BP} + f_W \quad (1)$$

The regression model we developed in this study (Equation (S1)), parallels that of Equation (1). We can therefore compare patterns in the regression coefficients with distribution coefficients estimated empirically by other means. Experimental measurements confirm that PFASs can be incorporated into phospholipid bilayers and that the strength of these interactions differs according to carbon-chain length and functional group.<sup>18, 33, 40</sup> In fact, all estimates of  $K_{PL,W}$  increase with carbon chain-length,<sup>13, 17, 38</sup> which is consistent with the increase in association by chain-length observed in this study (Figure 3).

Several studies report a curvilinear relationship between chain length and protein water association constants ( $K_{PW}$ ). Literature estimates of  $K_{PW}$  based on albumin affinity show peak binding affinity in PFCAs with anywhere from seven (PFHpA) to nine (PFNA) carbons.<sup>27–29</sup> A similar peak in protein association for PFNA is observed in this study, although the protein measurement reported here represents total proteins (Figure 3). Albumin is found in the blood and while we were unable to obtain paired blood samples from these whales, associations with L-FABP show a similar non-monotonic relationship between chain-length and binding affinity with a maximum occurring at 11 carbons (PFUnDA).<sup>26</sup> Figure 2B shows the relative proportion of PFASs in liver peaks at PFUnDA, which is consistent with the binding affinities for L-FABP.

PFASs can also be transported by organic anion transporters (OATs) and organic anion transporting polypeptides (OATPs), which control reabsorption of organic anions from urine in the kidney.<sup>41–43</sup> These transporter proteins as well as Na<sup>+</sup>/taurocholate co-transporting polypeptide (NTCP) have also been shown to be important for mediating uptake of PFASs in the liver.<sup>44</sup> In contrast, the brain has very low levels of transporter proteins and may therefore reflect PFASs that are more passively permeable. Variability in PFAS affinities for specific proteins may therefore account for the additional variability not explained by the phospholipid associations modeled in Table 1 and should be explored in future work.

The protein measures presented here represent total protein and do not distinguish among specific proteins that have been associated with PFASs. Relatedly, the presence of residual whole blood in the tissue samples may obscure the interpretation of some of the results such as the lack of significant difference in total proteins across many of the tissues (Figure 1C),

or the distinct results observed for brain measurements (Table 1). Future studies may wish to concurrently measure specific proteins and PFASs to further clarify the role of proteins. Despite these limitations, the significant associations with phospholipids observed in this study point to their importance for accumulation of PFASs.

Our data are consistent with both protein and phospholipid accumulation for PFASs, and can be used to develop a broader model of bioaccumulation that incorporates these mechanisms. An improved mechanistic understanding of factors affecting tissue accumulation of legacy PFASs can inform management strategies for replacement compounds that exhibit similar properties. Many of the PFASs measured here will not degrade in the environment, and they have continued to be present in marine biota long after product phase-outs.<sup>45</sup> Understanding the mechanisms that drive the accumulation of PFASs in biological systems is critical for mitigating risks of legacy PFASs and predicting the future behavior of the much wider class of replacement compounds.

## Supplementary Material

Refer to Web version on PubMed Central for supplementary material.

## Acknowledgements

We acknowledge financial support for this study from the National Institute for Environmental Health Sciences (P42ES027706) Superfund Research Center and the Smith Family Foundation. CD acknowledges a STAR graduate fellowship from the U.S. Environmental Protection Agency (F13D10739). We thank Maria Dam (Environment Agency, Faroe Islands) for assistance with pilot whale sample selection.

## References

1. ATSDR, Toxicological Profile for Perfluoroalkyls; U.S. Department of Health and Human Services, Public Health Service: Atlanta, GA, 2018.
2. Sunderland EM; Hu XC; Dassuncao C; Tokranov AK; Wagner CC; Allen JG, A review of the pathways of human exposure to poly- and perfluoroalkyl substances (PFASs) and present understanding of health effects. *J Exposure Sci Environ Epidemiol*, 2018, DOI: 10.1038/s41370-018-0094-1.
3. Kelly BC; Ikonomou MG; Blair JD; Surridge B; Hoover D; Grace R; Gobas FAPC, Perfluoroalkyl Contaminants in an Arctic Marine Food Web: Trophic Magnification and Wildlife Exposure. *Environ Sci Technol* 2009, 43, 4037–4043. [PubMed: 19569327]
4. Zhang X; Zhang Y; Dassuncao C; Lohmann R; Sunderland EM, North Atlantic Deep Water formation inhibits high Arctic contamination by continental perfluorooctanesulfonate discharges. *Global Biogeochem Cycles* 2017, 31, 1332–1343.
5. Dassuncao C; Hu XC; Nielsen F; Weihe P; Grandjean P; Sunderland EM, Shifting Global Exposures to Poly- and Perfluoroalkyl Substances (PFASs) Evident in Longitudinal Birth Cohorts from a Seafood-Consuming Population. *Environ Sci Technol* 2018, 52, 3738–3747. [PubMed: 29516726]
6. Arnot JA; Gobas FAPC, A review of bioconcentration factor (BCF) and bioaccumulation factor (BAF) assessments for organic chemicals in aquatic organisms. *Environ Rev (Ottawa, ON, Can)* 2006, 14, 257–297.
7. Conder JM; Hoke RA; Wolf W d.; Russell, M. H.; Buck, R. C., Are PFCAs Bioaccumulative? A Critical Review and Comparison with Regulatory Criteria and Persistent Lipophilic Compounds. *Environ Sci Technol* 2008, 42, 995–1003. [PubMed: 18351063]

8. Armitage JM; Arnot JA; Wania F, Potential role of phospholipids in determining the internal tissue distribution of perfluoroalkyl acids in biota. *Environ Sci Technol* 2012, 46, 12285–12286. [PubMed: 23134198]
9. Ng CA; Hungerbuhler K, Bioconcentration of perfluorinated alkyl acids: how important is specific binding? *Environ Sci Technol* 2013, 47, 7214–7223. [PubMed: 23734664]
10. Shi Y; Vestergren R; Nost TH; Zhou Z; Cai Y, Probing the Differential Tissue Distribution and Bioaccumulation Behavior of Per- and Polyfluoroalkyl Substances of Varying Chain-Lengths, Isomeric Structures and Functional Groups in Crucian Carp. *Environ Sci Technol* 2018, 52, 4592–4600. [PubMed: 29611424]
11. Greaves AK; Letcher RJ; Sonne C; Dietz R; Born EW, Tissue-specific concentrations and patterns of perfluoroalkyl carboxylates and sulfonates in East Greenland polar bears. *Environ Sci Technol* 2012, 46, 11575–11583. [PubMed: 23057644]
12. Ahrens L; Siebert U; Ebinghaus R, Total body burden and tissue distribution of polyfluorinated compounds in harbor seals (*Phoca vitulina*) from the German Bight. *Mar Pollut Bull* 2009, 58, 520–525. [PubMed: 19121527]
13. Armitage JM; Arnot JA; Wania F; Mackay D, Development and evaluation of a mechanistic bioconcentration model for ionogenic organic chemicals in fish. *Environ Toxicol Chem* 2013, 32, 115–128. [PubMed: 23023933]
14. Fujikawa M; Nakao K; Shimizu R; Akamatsu M, The usefulness of an artificial membrane accumulation index for estimation of the bioconcentration factor of organophosphorus pesticides. *Chemosphere* 2009, 74, 751–757. [PubMed: 19084258]
15. Bittermann K; Spycher S; Endo S; Pohler L; Huniar U; Goss KU; Klamt A, Prediction of Phospholipid-Water Partition Coefficients of Ionic Organic Chemicals Using the Mechanistic Model COSMOmic. *J Phys Chem B* 2014, 118, 14833–14842. [PubMed: 25459490]
16. Chen F; Gong Z; Kelly BC, Bioaccumulation Behavior of Pharmaceuticals and Personal Care Products in Adult Zebrafish (*Danio rerio*): Influence of Physical-Chemical Properties and Biotransformation. *Environ Sci Technol* 2017, 51, 11085–11095. [PubMed: 28853873]
17. Droge STJ, Membrane-water partition coefficients to aid risk assessment of perfluoroalkyl anions and alkyl sulfates. *Environ Sci Technol* 2019, 53, 760–770. [PubMed: 30572703]
18. Fitzgerald NJM; Wargenau A; Sorenson C; Pedersen J; Tufenkji N; Novak PJ; Simcik MF, Partitioning and Accumulation of Perfluoroalkyl Substances in Model Lipid Bilayers and Bacteria. *Environ Sci Technol* 2018, 52, 10433–10440. [PubMed: 30148610]
19. Weber AK; Barber LB; LeBlanc DR; Sunderland EM; Vecitis CD, Geochemical and Hydrologic Factors Controlling Subsurface Transport of Poly- and Perfluoroalkyl Substances, Cape Cod, Massachusetts. *Environ Sci Technol* 2017, 51, 4269–4279. [PubMed: 28285525]
20. Zhang X; Lohmann R; Dassuncao C; Hu XC; Weber AK; Vecitis CD; Sunderland EM, Source attribution of poly- and perfluoroalkyl substances (PFASs) in surface waters from Rhode Island and the New York Metropolitan Area. *Environ Sci Technol Lett* 2016, 3, 316–321. [PubMed: 28217711]
21. Bradford MM, A rapid and sensitive method for the quantitation of microgram quantities of protein utilizing the principle of protein-dye binding. *Anal Biochem* 1976, 72, 248–254. [PubMed: 942051]
22. Folch J; Lees M; Stanley GHS, A simple method for the isolation and purification of total lipids from animal tissues. *J Biol Chem* 1956, 226, 497–509.
23. Wang J; Pan Y; Cui Q; Yao B; Wang J; Dai J, Penetration of PFASs Across the Blood Cerebrospinal Fluid Barrier and Its Determinants in Humans. *Environ Sci Technol* 2018, 52, 13553–13561. [PubMed: 30362723]
24. Luebker DJ; Hansen KJ; Bass NM; Butenhoff JL; Seacat AM, Interactions of fluorochemicals with rat liver fatty acid-binding protein. *Toxicology* 2002, 176, 175–185. [PubMed: 12093614]
25. Woodcroft MW; Ellis DA; Rafferty SP; Burns DC; March RE; Stock NL; Trumpour KS; Yee J; Munro K, Experimental characterization of the mechanism of perfluorocarboxylic acids' liver protein bioaccumulation: the key role of the neutral species. *Environ Toxicol Chem* 2010, 29, 1669–1677. [PubMed: 20821618]



26. Zhang L; Ren XM; Guo LH, Structure-based investigation on the interaction of perfluorinated compounds with human liver fatty acid binding protein. *Environ Sci Technol* 2013, 47, 11293–11301. [PubMed: 24006842]
27. Hebert PC; MacManus-Spencer LA, Development of a Fluorescence Model for the Binding of Medium- to Long-Chain Perfluoroalkyl Acids to Human Serum Albumin Through a Mechanistic Evaluation of Spectroscopic Evidence. *Anal Chem* 2010, 82, 6463–6471. [PubMed: 20590160]
28. MacManus-Spencer LA; Tse ML; Hebert PC; Bischel HN; Luthy RG, Binding of perfluorocarboxylates to serum albumin: a comparison of analytical methods. *Anal Chem* 2009, 82, 974–981.
29. Bischel HN; Macmanus-Spencer LA; Zhang C; Luthy RG, Strong associations of short-chain perfluoroalkyl acids with serum albumin and investigation of binding mechanisms. *Environ Toxicol Chem* 2011, 30, 2423–2430. [PubMed: 21842491]
30. Dauchy X; Boiteux V; Bach C; Rosin C; Munoz JF, Per- and polyfluoroalkyl substances in firefighting foam concentrates and water samples collected near sites impacted by the use of these foams. *Chemosphere* 2017, 183, 53–61. [PubMed: 28531559]
31. Houtz EF; Sutton R; Park JS; Sedlak M, Poly- and perfluoroalkyl substances in wastewater: Significance of unknown precursors, manufacturing shifts, and likely AFFF impacts. *Water Res* 2016, 95, 142–149. [PubMed: 26990839]
32. Houtz EF; Sedlak DL, Oxidative conversion as a means of detecting precursors to perfluoroalkyl acids in urban runoff. *Environ Sci Technol* 2012, 46, 9342–9349. [PubMed: 22900587]
33. Nouhi S; Ahrens L; Campos Pereira H; Hughes AV; Campana M; Gutfreund P; Palsson GK; Vorobiev A; Hellsing MS, Interactions of perfluoroalkyl substances with a phospholipid bilayer studied by neutron reflectometry. *J Colloid Interface Sci* 2018, 511, 474–481. [PubMed: 29073553]
34. Wang X; Li B; Zhao WD; Liu YJ; Shang DS; Fang WG; Chen YH, Perfluorooctane sulfonate triggers tight junction “opening” in brain endothelial cells via phosphatidylinositol 3-kinase. *Biochem Biophys Res Commun* 2011, 410, 258–63. [PubMed: 21651890]
35. Berntsen HF; Bjorklund CG; Audinot JN; Hofer T; Verhaegen S; Lentzen E; Gutleb AC; Ropstad E, Time-dependent effects of perfluorinated compounds on viability in cerebellar granule neurons: Dependence on carbon chain length and functional group attached. *Neurotoxicology* 2017, 63, 70–83. [PubMed: 28919516]
36. Eggers Pedersen K; Basu N; Letcher R; Greaves AK; Sonne C; Dietz R; Styrisshave B, Brain region-specific perfluoroalkylated sulfonate (PFSA) and carboxylic acid (PFCA) accumulation and neurochemical biomarker responses in east Greenland polar bears (*Ursus maritimus*). *Environ Res* 2015, 138, 22–31. [PubMed: 25682255]
37. Ng CA; Hungerbuhler K, Bioaccumulation of perfluorinated alkyl acids: observations and models. *Environ Sci Technol* 2014, 48, 4637–4648. [PubMed: 24762048]
38. Bittermann K; Linden L; Goss KU, Screening tools for the bioconcentration potential of monovalent organic ions in fish. *Environ Sci: Processes Impacts* 2018, 20, 845–853.
39. Goss KU; Bittermann K; Henneberger L; Linden L, Equilibrium biopartitioning of organic anions - A case study for humans and fish. *Chemosphere* 2018, 199, 174–181. [PubMed: 29438944]
40. Matyszewska D; Tappura K; Orädd G; Bilewicz R, Influence of perfluorinated compounds on the properties of model lipid membranes. *J Phys Chem B* 2007, 111, 9908–9918. [PubMed: 17672485]
41. Nakagawa H; Hirata T; Terada T; Jutabha P; Miura D; Harada KH; Inoue K; Anzai N; Endou H; Inui KI; Kanai Y, Roles of organic anion transporters in the renal excretion of perfluorooctanoic acid. *Basic Clin Pharmacol Toxicol* 2008, 103, 1–8. [PubMed: 18373647]
42. Weaver YM; Ehresman DJ; Butenhoff JL; Hagenbuch B, Roles of rat renal organic anion transporters in transporting perfluorinated carboxylates with different chain lengths. *Toxicol Sci* 2010, 113, 305–314. [PubMed: 19915082]
43. Yang CH; Glover KP; Han X, Organic anion transporting polypeptide (Oatp) 1a1-mediated perfluorooctanoate transport and evidence for a renal reabsorption mechanism of Oatp1a1 in renal elimination of perfluorocarboxylates in rats. *Toxicol Lett* 2009, 190, 163–171. [PubMed: 19616083]

44. Zhao W; Zitzow JD; Ehresman DJ; Chang SC; Butenhoff JL; Forster J; Hagenbuch B, Na<sup>+</sup>/Taurocholate Cotransporting Polypeptide and Apical Sodium-Dependent Bile Acid Transporter Are Involved in the Disposition of Perfluoroalkyl Sulfonates in Humans and Rats. *Toxicol Sci* 2015, 146, 363–373. [PubMed: 26001962]
45. Dassuncao C; Hu XC; Zhang X; Bossi R; Dam M; Mikkelsen B; Sunderland EM, Temporal Shifts in Poly- and Perfluoroalkyl Substances (PFASs) in North Atlantic Pilot Whales Indicate Large Contribution of Atmospheric Precursors. *Environ Sci Technol* 2017, 51, 4512–4521. [PubMed: 28350446]

Author Manuscript

Author Manuscript

Author Manuscript

Author Manuscript

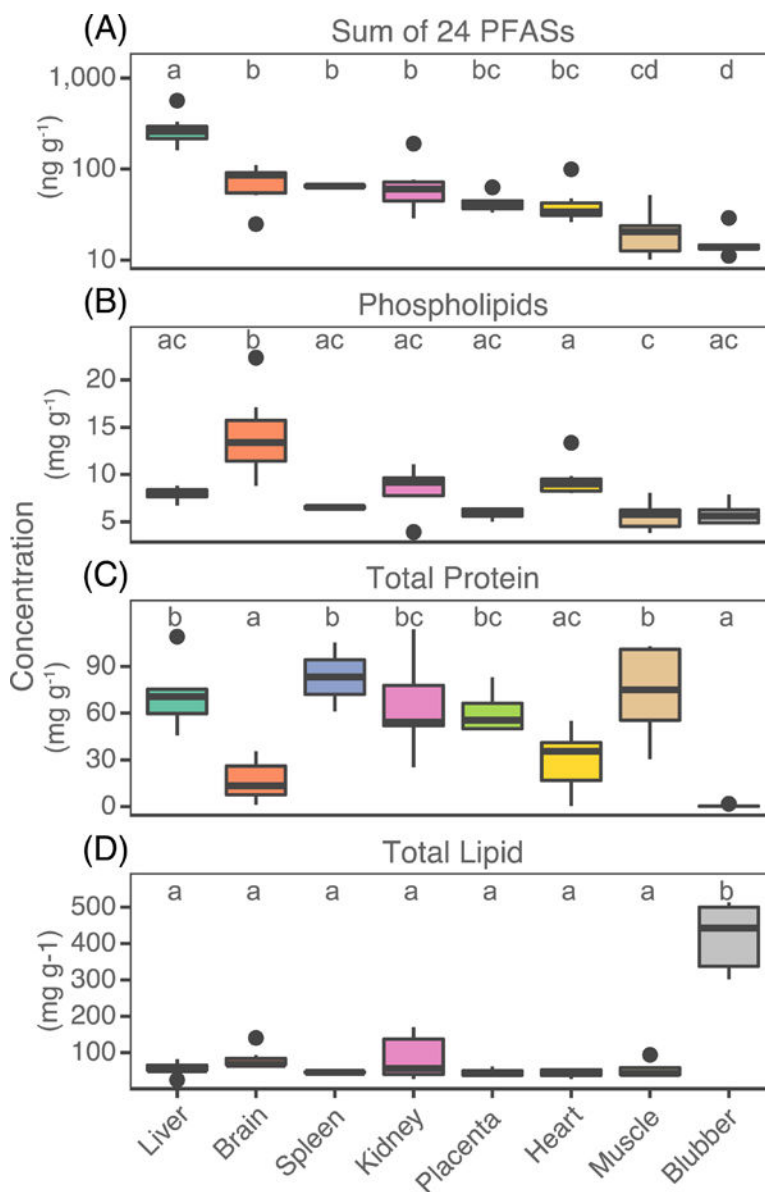


**Figure 1.** Measured concentrations of (A) the sum of 24 PFASs, (B) phospholipids, (C) total protein, and (D) total lipid in each pilot whale tissue. The dark line within the box represents the median, box hinges represent the first and third quartile, the whiskers represent 1.5 the interquartile range, and black points are outliers. Common letters above each box indicate tissues with no significant difference in between group comparisons using Tukey's test.

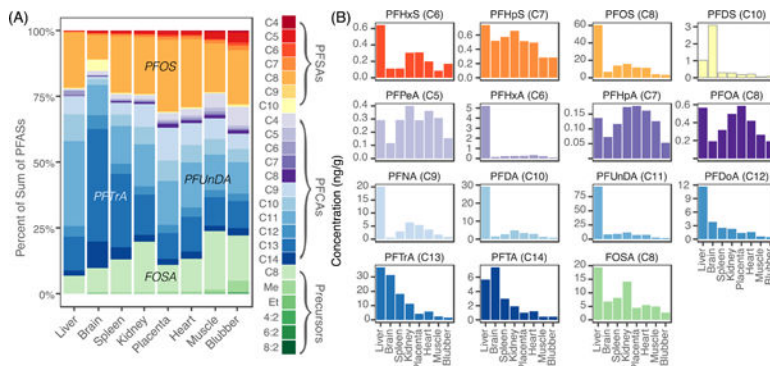


**Figure 2.** Distribution of PFASs measured in pilot whale tissues. Panel (A) shows the average composition of 24 PFASs within each tissue. PFCAs and PFSA's are indicated by carbon number (C4-C14), the precursors FOSA as C8, MeFOSAA as Me, EtFOSAA as Et, and fluorotelomer sulfonates by their carbon numbers. Panel (B) shows the relative distribution of each PFAS across tissues. Compounds shown in (A) but not shown in (B) were infrequently detected (<15%).

Author Manuscript

Author Manuscript

Author Manuscript

Author Manuscript

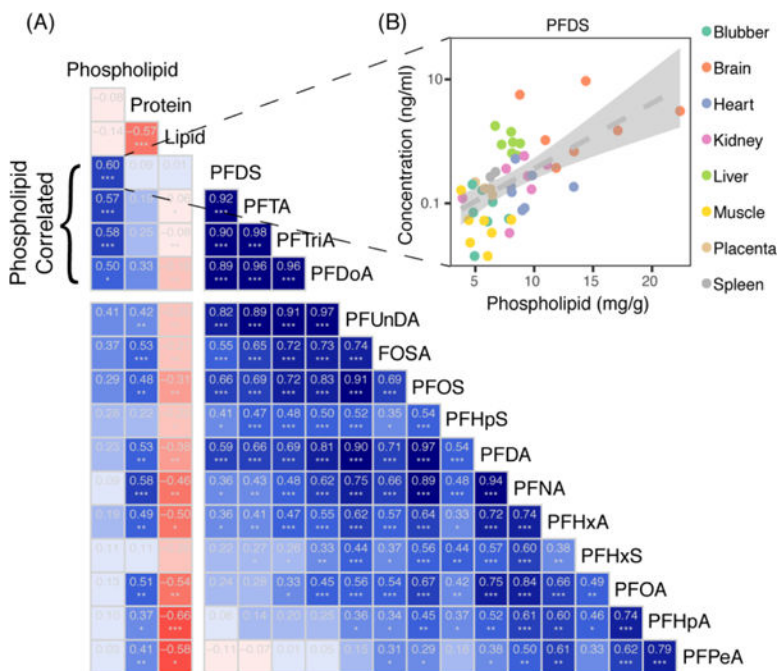


**Figure 3.** (A) Spearman correlations ( $r_s$ ) between measured compounds across whale tissues ordered and grouped by degree of correlation. The intensities of blue and red show the strength of positive and negative correlations, respectively. Significant correlations are denoted by asterisks (\* indicates  $p < 0.05$ ; \*\* indicates  $p < 0.005$ , \*\*\* indicates  $p < 0.0005$ ). (B) An example of the measured data underlying the correlation between phospholipids and PFDS.

**Table 1.**

Results of mixed-effects regression models showing percent change in PFAS concentration for each mg g<sup>-1</sup> increase in phospholipid, protein, or lipid concentration

PFAS	C#	Model with all tissues						Model without brain <sup>a</sup>					
		PL	<i>p</i>	Protein	<i>p</i>	Lipid	<i>p</i>	PL	<i>p</i>	Protein	<i>p</i>	Lipid	<i>p</i>
PFDS	10	26%	<0.001	-	-	-	-	20%	0.043	-	-	-	-
PFTA	14	22%	<0.001	0.9%	0.049	-	-	19%	<0.001	1.2%	0.007	-	-
PFTTrA	13	23%	<0.001	1.3%	0.006	-	-	23%	<0.001	1.6%	0.001	-	-
PFDoA	12	17%	0.001	1.3%	0.005	-	-	22%	0.017	1.5%	0.004	-	-
PFUnDA	11	12%	0.025	1.8%	0.001	-	-	24%	0.025	1.8%	0.003	-	-
PFDA	10	-	-	1.7%	0.001	-	-	24%	0.017	1.7%	0.002	-	-
PFOS	8	-	-	1.4%	0.002	-	-	25%	0.007	1.4%	0.003	-	-
FOSA	8	8.5%	0.005	1.3%	<0.001	-	-	19%	<0.001	1.3%	<0.001	-	-
PFNA	9	-	-	2.0%	<0.001	-	-	23%	0.007	1.6%	0.001	-	-
PFOA	8	-	-	1.0%	0.001	-	-	12%	0.003	0.6%	0.005	-	-
PFHxS	6	-	-	-	-	-	-	19%	0.034	-	-	-	-
PFHpA	7	-	-	1%	<0.001	-	-	-	-	-	-	-0.3%	<0.001
PFHxA	6	-	-	1%	0.025	-	-	22%	0.023	-	-	-	-
PFPeA	5	-	-	1%	0.006	-	-	15%	<0.001	-	-	-	-

<sup>a</sup>Performed as a sensitivity analysis to test for confounding by brain specific processes such as the effects of the blood-brain barrier.